$Li_3[ScN_2]$: The First Nitridoscandate(III)—Tetrahedral Sc Coordination and Unusual MX_2 Framework

Rainer Niewa,* Dmitri A. Zherebtsov, and Stefano Leoni[a]

Abstract: $Li_3[ScN_2]$ was prepared from Li_3N with Sc or ScN in a nitrogen atmosphere at 1020 K as a light yellow powder with an optical band gap of about 2.9 eV. The crystal structure was refined based on X-ray and neutron powder diffraction data ($Ia\bar{3}$, $Z = 16$, X-ray diffraction: $R_{profile} = 0.078$, $R_{Bragg} = 0.070$; Neutron diffraction: $R_{profile} = 0.077$, $R_{Bragg} = 0.074$; Rietfeld: $a = 1003.940(8)$ pm, Guinier: $a = 1004.50(3)$ pm). $Li_3[ScN_2]$ is an isotype of $Li_3[AlN_2]$ and $Li_3[GaN_2]$ and crystallizes in an ordered superstructure of the Li_2O structure type, leading to a three-dimensional framework of all-vertex-sharing tetrahedra $^3_\infty[ScN^{3-}_{4/2}]$. Li is displaced from the center of a tetrahedron of N atoms in the direction of one trigonal face. $Li_3[ScN_2]$ decomposes above 1050 K to form ScN and Li_3N. Calculations of the periodic nodal surface (PNS) and of the electron localization function (ELF) support the picture of a covalent Sc–N network separated from isolated Li cations, whereby scandium d orbitals are involved in the chemical bonding.

Keywords: bond theory · ELF (electron localization function) · lithium · nitrides · scandium

Introduction

In the last decade there has been a renewed interest in the chemistry of nitrides and nitridometalates.[1–3] Within this field of interest, the nitride chemistry of rare-earth metals, in particular, is still comparable undeveloped.[4] The known rare-earth compounds can be loosely classified according to the following:

1) Metal-rich compounds with an often variable nitrogen content, for example, compositions as anti-perovskite phases $(R_3N)M$ (R = rare-earth metal, M = main group metal),[5, 6] or $RT_{12}N_x$, $R_2T_{17}N_x$, and $R_3T_{29}N_x$ (T = transition metal),[7] which are currently under intensive investigation world-wide due to the superior hard-magnetic properties.
2) Nitridoborates, nitridosilicates[8–10] and nitridometalates of d elements, for example, $Ce_2[CrN_3]$,[11] $Ce_2[MnN_3]$,[12, 13] and $R_3[T_2N_6]$ (R = La, Ce, Pr; T = Nb, Ta),[14] with the rare-earth metal serving as an electropositive component.
3) Interestingly, only few compounds with the alkali and alkaline-earth metals are known: from lanthanum a defect rocksalt nitride phase $(Ca_xLa_{1-x})N_{1-x/3}$ $(0 < x < 0.7)$ was reported.[15] Cerium forms the disordered rocksalt phases $(CaCe^{IV})N_2$ and HT-$(SrCa^{IV})N_2$, the α-$NaFeO_2$-type LT-$SrCe^{IV}N_2$,[16] and $BaCe^{IV}N_2$, which crystallizes in the layered β-$RbScO_2$ structure.[17] Though, there are some indications for a homogeneity range of HT-$SrCeN_2$ in the sense of a solid solution with CeN,[16] all these compounds contain Ce^{4+}. Similar is the situation with lithium: only $Li_2Ce^{IV}N_2$ with an ordered *anti*-La_2O_3 structure has been reported so far.[18]

Scandium, as the lighter homologue of La in the periodic table, in many respects behaves similarly to both the rare-earth metals and to aluminum. At the same time it connects to the 3d transition metal series. In inorganic nitride chemistry, only the binary ScN, the ternary $ScNbN_{1-x}$ and $ScTaN_{1-x}$, and some solid solution phases of ScN with other binary nitrides are known so far.[19–21] Here we report on the new compound $Li_3[ScN_2]$, prepared from Li_3N and ScN or Sc in a nitrogen atmosphere.

Results and Discussion

$Li_3[ScN_2]$ was prepared from Li_3N and ScN fine powders in nitrogen atmosphere in preference over the reaction of Li_3N with Sc. In the latter case, typically, large amounts of unreacted Sc remained due to kinetic hindrance by slow diffusion in the larger Sc grains. Under the conditions of thermal analyses in an Ar atmosphere $Li_3[ScN_2]$ decomposes at temperatures above 1050 K to give a single-phase brownish powder of δ-ScN (see Figure 1). Li_3N sublimes to the colder parts of the apparatus. The mass loss of 35.4 % agrees with the calculated value of 37.1 % for the loss of 1 mol Li_3N per formula unit. A kink in the TG (thermogravimetry) curve followed by a slower mass loss at higher temperatures indicates a reduction of the powder surface, presumably by formation of a melt. The thermal effect at $T_{onset} = 1090$ K

[a] Dr. R. Niewa, Dr. D. A. Zherebtsov, Dr. S. Leoni
Max-Planck-Institut für Chemische Physik fester Stoffe
Nöthnitzer Strasse 40, 01187 Dresden (Germany)
Fax: (+49) 351-46463002
E-mail: niewa@cpfs.mpg.de

 DOI: 10.1002/chem.200304986

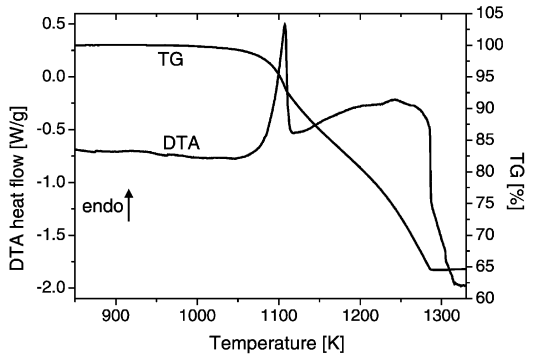

Figure 1. DTA/TG diagram of the decomposition of $Li_3[ScN_2]$ in an Ar atmosphere (heating rate 10 K min^{-1}).

coincides with the melting point of Li_3N (1086 K). The mass loss already slowly starts at temperatures below the melting point, corresponding to the significant vapour pressure of Li_3N at elevated temperatures. Thus, the thermal peak is interpreted as melting point of Li_3N formed in the decomposition reaction. This interpretation was confirmed by samples $Li_3[ScN_2]$ quenched from different temperatures and composed of various amounts of $Li_3[ScN_2]$, α-Li_3N, and δ-ScN depending on the thermal history. The behavior of $Li_3[AlN_2]$ and $Li_3[GaN_2]$[22] is similar (decomposition above 1270 K and 1070 K to form AlN and LiGa, respectively).

The crystal structure of $Li_3[ScN_2]$ was refined based on X-ray and neutron powder diffraction data to locate all atoms reliably. Figure 2 depicts the refinement results. $Li_3[ScN_2]$ is an isotype of $Li_3[AlN_2]$ and $Li_3[GaN_2]$[22, 23] and crystallizes in

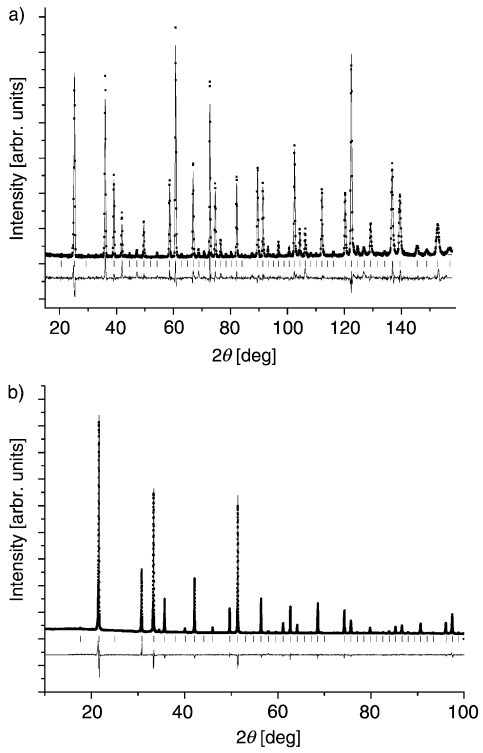

Figure 2. a) Neutron and b) X-ray diffraction patterns ($Cu_{K\alpha 1}$ radiation) of $Li_3[ScN_2]$ (dots), fitted profile (line), and difference curve (below). Tick marks indicate the positions of possible Bragg reflections.

a $2 \times 2 \times 2$ superstructure of Li_2O. An ordered occupation of the tetrahedral holes with Sc and Li in the face-centered cubic (fcc) arrangement of the N atoms leads to a three-dimensional framework of all-vertex-sharing tetrahedra $^3_\infty[ScN^{3-}_{4/2}]$ as is shown in Figure 3. The Sc atoms are located in a nearly

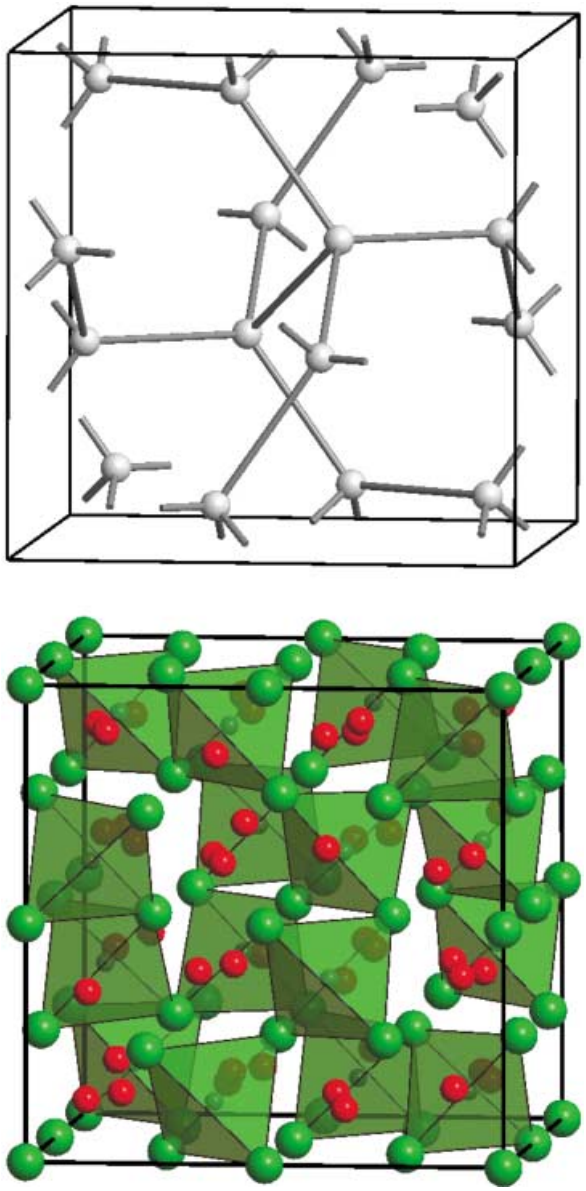

Figure 3. Comparison of the Si network of γ-Si[38] (top) and the $^3_\infty[ScN^{3-}_{4/2}]$ network (green hollow tetrahedra) in $Li_3[ScN_2]$ (red: Li) (bottom). One cubic unit cell is shown.

regular tetrahedron of N atoms. To our knowledge any tetrahedral coordination of Sc in purely inorganic compounds is unknown so far. In coordination compounds only few examples with strongly distorted tetrahedra ScN_2Te_2, $Sc(OAr)_4$, ScN_3C, and ScN_3O with sizeable ligands have been observed.[24–27] The bond lengths in the range of d(Sc–N) = 210.7(1) – 212.5(1) pm in $Li_3[ScN_2]$ are slightly shorter than the corresponding bond lengths in the binary δ-ScN compound with Sc in octahedral coordination (d(Sc–N)

≈225 pm). In coordination compounds the Sc–N bond lengths usually fall in the range of 204–220 pm.[26–29] The Li atom is displaced from the center of the nitrogen tetrahedra towards one trigonal face, as indicated by three shorter distances $d(\mathrm{Li–N}) = 209.7(6)$, 210.6(6), and 222.8(6) pm, which are in the range expected for Li in tetrahedral or trigonal planar coordination by N,[1–3] and one longer distance $d(\mathrm{Li–N}) = 245.6(6)$ pm. For comparison the distance $d(\mathrm{Li–N}) = 210.6$ pm was determined for the trigonal planar coordinated Li site in Li_3N.[30] Figure 4 depicts the coordination environments of Sc and Li. A similar situation was observed, for example, for LiCaN,[31] whereby the larger Ca^{2+} ion requires an expansion of the fcc arrangement of nitrogen accompanied by a distortion of the cubic symmetry to an orthorhombic unit cell.

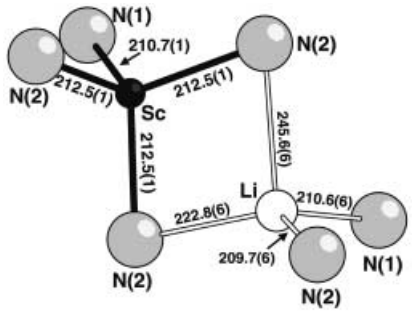

Figure 4. Coordination of the Sc and Li sites in $Li_3[ScN_2]$. While Sc is surrounded by a nearly ideal tetrahedron, Li is displaced from the center of a tetrahedron towards one trigonal face. Distances are given in pm, standard deviations of the last digit in parentheses.

The title compound fits well within the row of third-period Li nitrides in their highest observed oxidation states: LiMgN,[23, 32] LiZnN,[23] $Li_3[ScN_2]$, $Li_5TiN_3 \equiv Li_3[(Li_{1-x}Ti_x)N_2]$ $(x = 2/3)$,[33] $Li_7[VN_4]$,[34] $Li_6[CrN_4]$,[35] $Li_7[MnN_4]$,[36] $Li_3[FeN_2]$.[37] The compounds $Li_3[ScN_2]$ and $Li_3[FeN_2]$ with the same formula type realize different structures. The iron-containing compound crystallizes with a Li_2O-type (super)-structure with Fe occupying edge-sharing tetrahedra leading to infinite chains of $^3_\infty[FeN^{3-}_{4/2}]$.

Focussing on the $^3_\infty[ScN^{3-}_{4/2}]$ framework, the Sc arrangement is topologically equivalent to the Si arrangement in (high-pressure, high-density) γ-Si.[38] As for the isotypes $Li_3[AlN_2]$ and $Li_3[GaN_2]$, the introduction of nitrido ligands leads to an MX_2 framework for which, to our knowledge, no further example is known so far, neither for SiO_2 modifications nor for any aluminosilicate framework. As the Li_3N_2 substructure is isostructural with that of Mg_3N_2[39] and α-Ca_3N_2[40] (anti-bixbyite), the $^3_\infty[ScN^{3-}_{4/2}]$-framework consequently corresponds to the occupation of the unoccupied tetrahedral holes in the anti-bixbyite structure with Sc.

Though $Li_3[ScN_2]$ is an isotype of the long known $Li_3[AlN_2]$ and $Li_3[GaN_2]$, the previous crystal chemical discussion was focused on the Li_2O-type structure. To shed light on the topology of the unusual $^3_\infty[ScN^{3-}_{4/2}]$ network and on the nature of the Sc–N contacts, a periodic nodal surface (PNS)[41, 42] and the electron localization function (ELF)[43, 44] were calculated.

Periodic nodal surfaces are calculated from a Fourier summation of a few, for cubic symmetry frequently only one, Fourier coefficients. They appear as continuous, triply periodic surfaces, dividing three-dimensional space into two labyrinths that interpenetrate each other. For this property, they are very useful in understanding which topologies are compatible with a given space-group symmetry, and in elucidating the underlying structural motifs of a periodic arrangement of atoms. A diamond network, for example, will develop in one labyrinth of a periodic surface. Replacing the carbon atoms by tetrahedra ($MgCu_2$) or by very large aggregates of atoms (Mg_2Al_3) increases the structural complexity while keeping the topology constant.

The ELF is used to describe and visualize chemical bonds in solids and molecules. It compares the local Pauli repulsion of a given system with the one of a uniform electron gas of the same density. In physical space the ELF decomposes into basins. The way basins are related to each other through the definition domain of the ELF is a topological issue, which matches the topological information coded in the PNS. To illustrate this last point is also a task of this work.

The PNS (Figure 5) divides space into two labyrinths, one containing the Li positions and the other the Sc and N sites. As mentioned above the topology of the latter labyrinth corresponds to the network of γ-Si (space group $Ia\bar{3}$):[38] the Sc atoms build a point configuration of the same lattice complex as Si. The Sc–N network is thus a hierarchical derivative[45] of the Si network, whereby ScN_4 tetrahedra replace Si.

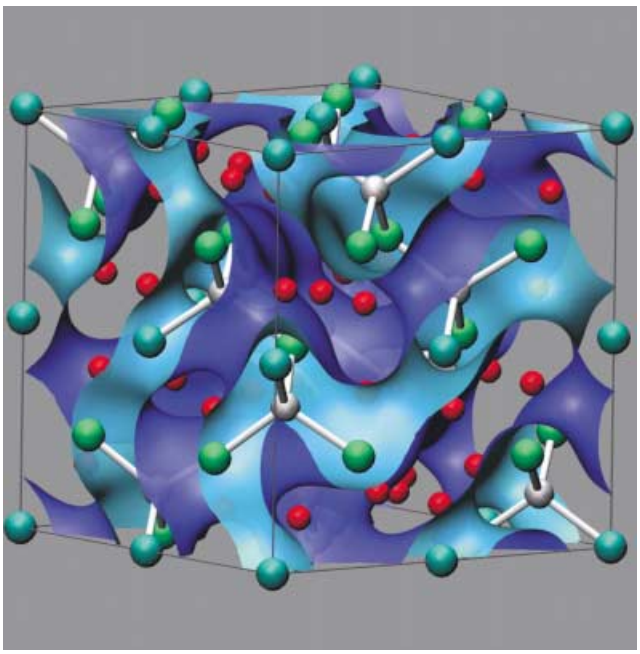

Figure 5. Unit cell of $Li_3[ScN_2]$. The $^3_\infty[ScN^{3-}_{4/2}]$ framework (Sc: white, N(1): green, N(2): dark green) is enclosed in one labyrinth of a PNS, while the Li atoms (red) are located in a second labyrinth (blue/dark blue surfaces).

Along the Sc–N connections, no ELF maxima are found (Figure 6). The outer-core basin set[46] of Sc decomposes into four basins for the interconnection value above $\eta_{ic} = 0.85$. The basin attractors point towards the faces of the N tetrahedra

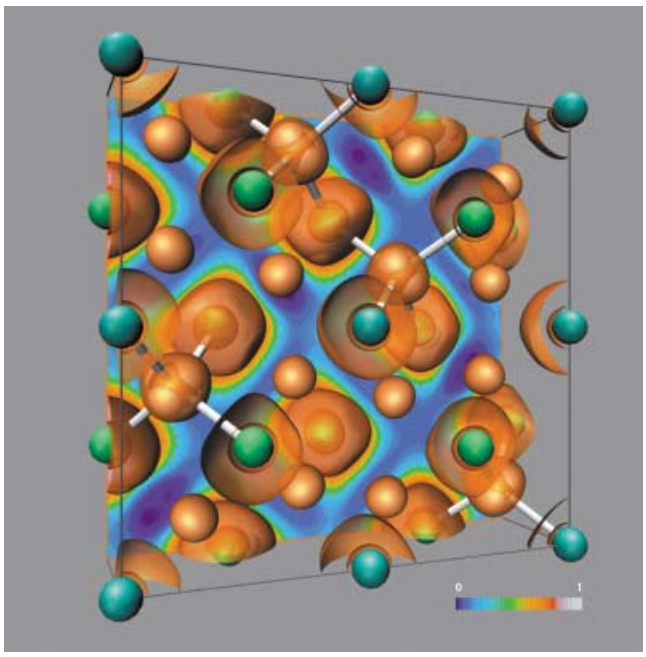

Figure 6. Section of the unit cell of $Li_3[ScN_2]$. Two isosurfaces of the ELF are displayed, showing the structuring of the outer-core localization domain of Sc (four light yellow maxima, opaque) and isolated Li atoms ($\eta_{ic} = 0.74$), and valence localization domains around N ($\eta_{ic} = 0.85$). An ELF slice through a nitrogen layer appears in the background.

around the Sc atom. The pronounced structuring of the outer-core localization domain hints at a participation of the scandium 3d orbitals in the bonding.[46] Choosing the interconnection ELF value of $\eta_{ic} = 0.15$, the outer-core basin set of the Sc atoms fuse with the valence basin sets of the N atoms, building one basin set of the ScN framework. At that value the basins of the lithium atoms are still isolated. This picture nicely corresponds with the analysis with PNS, in which Li^+ and the $^3_\infty[ScN^{3-}_{4/2}]$ framework are located in two different labyrinths.

Integration of the electronic density within the basins[47] provides supporting data for the analysis of the bonding situation. In the valence basin set of N, an excess of 2.5 e^- is found, and, by subtraction, Sc lacks 2 e^-. This together with the pronounced structuring of the localization domain at Sc is an indication for the participation of Sc in covalent chemical bonding and corresponds to the semiconducting/insulating property of the light yellow compound (optical band gap $\approx$2.9 eV, as determined by diffuse reflectivity).

With these values, the qualitative analysis of the ELF, and bearing in mind the separation operated by the PNS, two types of interaction can be distinguished: one substantially ionic (each Li atom transfers 1 e^- to the ScN framework), which develops across the PNS, and an Sc–N bonding interaction within one labyrinth of the nodal surface involving Sc 3d orbitals.

In summary, $Li_3[ScN_2]$ is the first nitridoscandate reported. For the first time Sc is observed in tetrahedral coordination in an inorganic compound. The $^3_\infty[ScN^{3-}_{4/2}]$ substructure comprises an unusual framework not observed in silicate chemistry.

Experimental Section

Materials: The sample handling, chemical analyses, and the preparation of Li_3N were carried out as described previously.[16] δ-ScN was produced from the elements (Sc: Hunan Institute of Rare-Earth Metals Materials (China); sublimed, dendritic, chemical analyses: $w(O) = 0.09(2)\,\%$, w(N, C) below determination limit $< 0.01\,\%$) within an induction furnace at $T_{max} = 1670$ K for 1 h. Chemical analyses of this δ-ScN resulted in $w(O) < 0.20(6)\,\%$, $w(N) = 23.3(6)\,\%$, $w(Sc) = 76.4(5)\,\%$, that is, $ScN_{0.98}O_{0.01}$, unit cell parameter $a = 450.35(2)$ pm.

$Li_3[ScN_2]$ can be obtained from α-Li_3N and Sc metal or from α-Li_3N and δ-ScN in nitrogen atmosphere at 1020 K. Best results were obtained with δ-ScN fine powders. The single-phase product was a light yellow, moisture sensitive powder that easily dissolved in hydrochloric acid (chemical analyses: $w(Li) = 22.4(2)\,\%$, $w(Sc) = 46.1(7)\,\%$, $w(O) < 0.10(2)\,\% = Li_{3.1}ScN_{2.2}$). A small amount of δ-ScN was indicated by two weak peaks in the powder XRD, excluded in the Rietfeld refinement.

Measurements: X-ray diffraction patterns were taken on an imaging plate Guinier camera.[16] The unit-cell parameter $a = 1004.50(3)$ pm was refined by least-squares fittings of X-ray powder data (CSD program package)[48] with LaB_6 as an internal standard ($a = 415.7$ pm). The neutron diffraction pattern was measured on diffractometer E9 at BENSC, HMI, Berlin (Germany). The sample container consisted of a V cylinder (diameter 8 mm, length 51 mm, wall thickness 0.15 mm) that was tightened by an In-sealing. Structure determination and combined refinements of the X-ray and neutron diffraction patterns succeeded in Fullprof:[49] X-ray diffraction, $Cu_{K\alpha 1}$ radiation, $15^\circ \le 2\theta \le 100^\circ$, 16640 profile points, $R_{profile} = 0.078$, $R_{Bragg} = 0.070$; neutron diffraction, $\lambda = 179.65(1)$ pm, $10^\circ \le 2\theta \le 156^\circ$, $R_{profile} = 0.077$, $R_{Bragg} = 0.074$, $a = 1003.940(8)$ pm, $Ia\bar{3}$, $Z = 16$; Sc in 16*c*, $x = 0.1222(1)$; Li in 48*e*, $x = 0.1576(5)$, $y = 0.3885(5)$, $z = 0.1095(7)$; N(1) in 8*a*; N(2) in 24*d*, $x = 0.2353(2)$, global $U_{iso} = 0.35(6) \times 10^2$ pm^2.

DTA/TG measurements (STA 449, NETZSCH, Ni crucibles, thermocouple type S, completely integrated into an argon-filled glove box) were performed under nitrogen and argon to analyze the formation of $Li_3[ScN_2]$, to find the optimum reaction conditions, and to examine the decomposition behavior. Temperature calibration was carried out with five melting points of pure metals. Above 1300 K the remaining decomposition product of $Li_3[ScN_2]$ was δ-ScN (chemical analyses: $w(Li) = 0.255(2)\,\%$, $w(Sc) = 75.1(8)\,\%$, $w(N) = 23.89(9)\,\%$, $w(O) = 0.48(4)\,\%$; $Li_{0.022}ScN_{1.021}O_{0.018}$).

The optical band gap was determined from diffuse reflection (Cary 500, prayingmantis, white standard $BaSO_4$, ratio 10:1) under inert conditions. The absorption energy was taken as the inflection point of the step-like decrease of the diffuse reflectivity.

Computational details: The PNS resulted from a short Fourier summation that included two reciprocal vector sets, (211,1,π) and (222,1,0), by following the method described in the literature.[41, 42] According to its definition,[41] the PNS is the isosurface of the Fourier summation at zero value.

For the calculation of the ELF, the one-electron Schrödinger equation was solved self-consistently within the LMTO scheme in the atomic sphere approximation. Interstitial empty spheres had to be added to correct for a large sphere overlap and to fill interstitial space. The basis sets consisted of 4s, 4p (down-folded), 3d for Sc, 2s, 2p (down-folded), 3d (down-folded) for Li, and 2s, 2p, 3d (down-folded) for N. The radii for the atoms and interstitial spheres were: $r(Sc) = 136.2$ pm, $r(Li) = 134.0$ pm, $r(N(1)) = 110.2$ pm, $r(N(2)) = 108.1$ pm, $r(E(1)) = 120.0$ pm, $r(E(2)) = 97.8$ pm, $r(E(3)) = 56.8$ pm. The ELF module of the TB-LMTO-ASA program[44] was used for the generation of the ELF grid. The final manipulation of the data was performed with the program Amira 2.3.[50]

Acknowledgement

The authors thank S. Hückmann and Dr. Yu. Prots for the collection of the X-ray diffraction data, U. Schmidt and B. Bayer for performing the chemical analyses, Dr. M. Kohout for valuable discussions, and Prof. Dr. R. Kniep for his constant interest and support. The optical band gap was determined by Dr. U. Schwarz and the neutron diffraction data was collected by Dr. G. Auffermann on the E9 diffractometer operated by Dr. D. Többens.

[1] R. Niewa, H. Jacobs, *Chem. Rev.* **1996**, *96*, 2053–2062.
[2] R. Kniep, *Pure Appl. Chem.* **1997**, *69*, 185–191.
[3] R. Niewa, F. J. DiSalvo, *Chem. Mater.* **1998**, *10*, 2733–2752.
[4] R. Marchand, in *Handbook on the Physics and Chemistry or Rare Earths*, *Vol. 25* (Eds.: K. A. Gschneidner, Jr., L. Eyring), North-Holland, Amsterdam, **1998**, pp. 51–99.
[5] H. Haschke, H. Nowotny, F. Benesovsky, *Monatsh. Chem.* **1967**, *98*, 2157–2163.
[6] M. Kirchner, W. Schnelle, F. R. Wagner, R. Niewa, *Solid State Sci.* in press.
[7] H. Fujii, H. Sun, in *Handbook of Magnetic Materials, Vol. 9* (Ed.: K. H. J. Buschow), North-Holland, Amsterdam, **1995**, pp. 304–404.
[8] P. Rogl, H. Klesnar, *J. Solid State Chem.* **1992**, *98*, 99–104.
[9] W. Schnick, H. Huppertz, *Chem. Eur. J.* **1997**, *3*, 679–683.
[10] M. Woike, W. Jeitschko, *Inorg. Chem.* **1995**, *34*, 5105–5108.
[11] S. Broll, W. Jeitschko, *Z. Naturforsch. Teil B* **1995**, *50*, 905–912.
[12] R. Niewa, G. V. Vajenine, F. J. DiSalvo, H. Luo, W. B. Yelon, *Z. Naturforsch. Teil B* **1998**, *53*, 63–74.
[13] R. Niewa, Z. Hu, C. Gracioli, U. Rößler, M. S. Golden, M. Knupfer, J. Fink, H. Giefers, G. Wortmann, F. M. F. de Groot, F. J. DiSalvo, *J. Alloys Compd.* **2002**, *346*, 129–133.
[14] L. Cario, Z. Gál, T. P. Braun, F. J. DiSalvo, B. Blaschkowski, H.-J. Meyer, *J. Solid State Chem.* **2001**, *162*, 90–95.
[15] S. J. Clarke, F. J. DiSalvo, *J. Solid. State Chem.* **1997**, *129*, 144–146.
[16] Y. Prots, R. Niewa, W. Schnelle, R. Kniep, *Z. Anorg. Allg. Chem.* **2002**, *628*, 1590–1596; Y. Prots, R. Niewa, W. Schnelle, *Z. Kristallogr. Suppl.* **2001**, *18*, 138.
[17] O. Seeger, J. Strähle, *Z. Naturforsch. Teil B* **1994**, *49*, 1169–1174.
[18] D. Halot, J. Flahaut, *C. R. Seances Acad. Sci. Ser. C* **1971**, *272*, 465–467.
[19] W. Lengauer, *J. Solid State Chem.* **1989**, *82*, 186–191.
[20] W. Lengauer, P. Ettmayer, *J. Less-Common Met.* **1988**, *141*, 157–162.
[21] For example: M. I. Aivazov, T. V. Rezchikova, *Zhur. Neo. Khimii* **1977**, *22*, 458–463; *Russ. J. Inorg. Chem.* **1977**, *22*, 250–253.
[22] R. Juza, *Angew. Chem.* **1948**, *60*, 74.
[23] R. Juza, F. Hund, *Z. Anorg. Allg. Chem.* **1948**, *257*, 13–25.
[24] L. K. Knight, W. E. Piers, R. McDonald, *Chem. Eur. J.* **2000**, *6*, 4322–4326.
[25] G. B. Deacon, P. E. Fanwick, A. Gitlits, I. P. Rothwell, B. W. Skelton, A. H. White, *Eur. J. Inorg. Chem.* **2001**, 1505–1514.
[26] M. Karl, K. Harms, G. Seybert, W. Massa, S. Fau, G. Frenking, K. Dehnicke, *Z. Anorg. Allg. Chem.* **1999**, *625*, 2055–2063.
[27] R. Anwander, O. Runte, J. Eppinger, G. Gerstberger, E. Herdtweck, M. Spiegler, *J. Chem. Soc. Dalton Trans.* **1998**, 847–858.
[28] J. S. Ghotra, M. B. Hursthouse, A. J. Welch, *J. Chem. Soc. Chem. Commun.* **1973**, 669–670.
[29] J. Arnold, C. G. Hoffman, D. Y. Dawson, F. J. Hollander, *Organometallics* **1993**, *12*, 3645–3654.
[30] A. Rabenau, H. Schulz, *J. Less-Common Met.* **1976**, *50*, 155–159.
[31] G. Cordier, A. Gudat, R. Kniep, A. Rabenau, *Angew. Chem.* **1989**, *101*, 1689–1690; *Angew. Chem. Int. Ed. Engl.* **1989**, *28*, 1702–1703.
[32] H. Yamane, T. H. Okabe, O. Ishiyama, Y. Waseda, M. Shimada, *J. Alloys Compd.* **2001**, *319*, 124–130; O. Hochrein, Ph.D. Thesis, TU-Darmstadt, **2001**.
[33] R. Juza, H. H. Weber, E. Meyer-Simon, *Z. Anorg. Allg. Chem.* **1953**, *273*, 48–64.
[34] R. Niewa, R. Kniep, *Z. Kristallogr. New Cryst. Struct.* **2001**, *216*, 5–6; R. Niewa, D. Zherebtsov, Z. Hu, *Inorg. Chem.* **2003**, *42*, 2538–2544.
[35] A. Gudat, S. Haag, R. Kniep, A. Rabenau, *Z. Naturforsch.* **1990**, *45*, 111–120.
[36] R. Juza, E. Anschütz, H. Puff, *Angew. Chem.* **1959**, *71*, 161; R. Niewa, F. R. Wagner, W. Schnelle, O. Hochrein, R. Kniep, *Inorg. Chem.* **2001**, *40*, 5215–5222.
[37] A. Gudat, R. Kniep, A. Rabenau, W. Bronger, U. Ruschewitz, *J. Less-Common Met.* **1990**, *161*, 31–36.
[38] R. H. Wentorf, Jr., J. S. Kasper, *Science* **1963**, *139*, 338–339.
[39] J. David, Y. Laurent, J. Lang, *Bull. Soc. Fr. Mineral.* **1971**, *94*, 340–346.
[40] Y. Laurent, J. Lang, M. T. le Bihan, *Acta Crystallogr. Sect. B* **1968**, *24*, 494–499.
[41] H. G. von Schnering, R. Nesper, *Z. Phys. B* **1991**, *83*, 407–412.
[42] S. Leoni, R. Nesper, *Acta Crystallogr. Sect. A* **2000**, *56*, 383–393.
[43] A. D. Becke, K. E. Edgecombe, *J. Chem. Phys.* **1990**, *92*, 5397–5403; A. Savin, O. Jepsen, J. Flad, O. K. Andersen, H. Preuss, H. G. von Schnering, *Angew. Chem.* **1992**, *104*, 186–188; *Angew. Chem. Int. Ed. Engl.* **1992**, *31*, 187–188.
[44] O. Jepsen, O. K. Andersen, The Stuttgart TB-LMTO-ASA Program, Version 4.7, Max-Planck-Institut für Festkörperforschung, Stuttgart, **2000**.
[45] W. Carrillo-Cabrera, N. Caroca-Canales, H. G. von Schnering, *Z. Anorg. Allg. Chem.* **1994**, 620, 247–257; M. O'Keeffe, M. Eddaoudi, H. Li, T. Reineke, O. M. Yagi, *J. Solid State Chem.* **2000**, *152*, 3–20.
[46] M. Kohout, F. R. Wagner, Yu. Grin, *Theor. Chem. Acc.* **2002**, *108*, 150–156.
[47] M. Kohout, Program Basin, Version 2.3, Max-Planck-Institut für Chemische Physik fester Stoffe, Dresden, **2001**.
[48] L. G. Akselrud, Yu. N. Grin, P. Y. Zavalii, V. K. Pecharsky, V. S. Fundamenski, *Z. Kristallogr. Suppl.* **1989**, *2*, 155; L. G. Akselrud, P. Y. Zavalii, Yu. N. Grin, V. K. Pecharsky, B. Baumgartner, E. Wölfel, *Mater. Sci. Forum* **1993**, *133–136*, 335–340.
[49] T. Roisnel, J. Rodriguez-Carvajal, WinPLOTR, Version May **2000**; J. Rodriguez-Carvajal, FULLPROF.2k, Version 1.6, **2000**, Laboratoire Léon Brillouin.
[50] Amira, Version 2.3, Zuse Institute Berlin (ZIB) and Indeed—Visual Concepts, Berlin, **2002**.

Received: March 25, 2003 [F4986]

